Supplementary Material

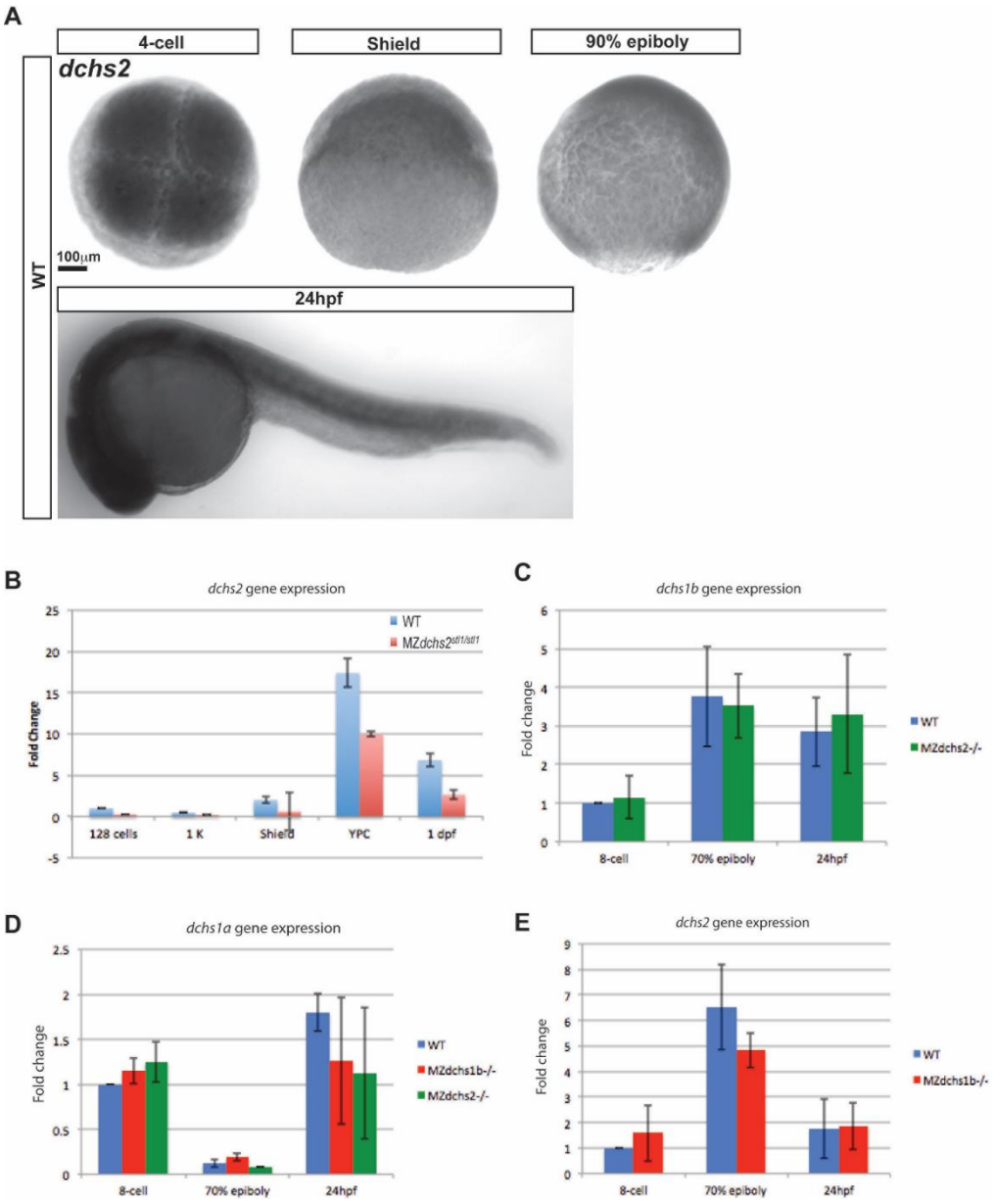

Figure S1 *dchs* expression in zebrafish

A. Whole-mount *in situ* hybridization of *dchs2* in WT embryos at 4-cell (1 hpf), shield (6 hpf), 90% epiboly (9 hpf), and 24 hpf stages.
B. Quantitative RT-PCR analysis of *dchs2* expression levels in MZ*dchs2*$^{stl1/stl1}$ mutants relative to WT embryos at maternal and zygotic stages.
C. Relative expression by qRT-PCR of *dchs1b* in WT and MZ*dchs1b*$^{stl1/stl1}$ embryos.
D. Relative expression by qRT-PCR of *dchs1a* in WT, MZ*dchs1b*$^{fh275/fh275}$, and MZ*dchs1b*$^{stl1/stl1}$ embryos.
E. Relative expression by qRT-PCR of *dchs2* in WT and MZ*dchs1b*$^{fh275/fh275}$ embryos.

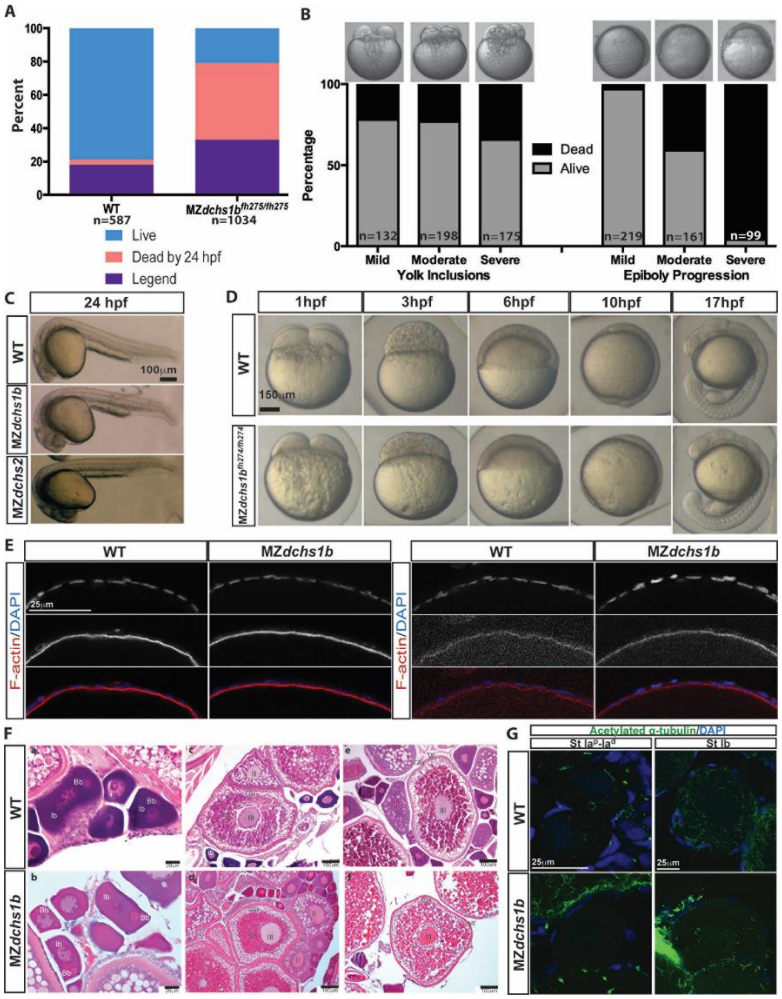

Figure S2. Survival, morphology, and histology of WT and *dchs* mutants

A. Survival and fertility for WT (n=587) and MZ*dchs1b*$^{fh275/fh275}$ (n= 1034) mutant embryos.
B. Survival of MZ*dchs1b*$^{fh275/fh275}$embryos based on severity of yolk inclusions and delayed epiboly phenotypes.
C. Morphology of WT, MZ*dchs1b*$^{fh275/fh275}$, and MZ*dchs1b*$^{stl1/stl1}$ embryos at 24 hpf.
D. Bright field images of WT and MZ*dchs1b*$^{fh27/fh274}$ time matched embryos at 1, 3, 6, 10, and 17 hpf.
E. Rhodamine phalloidin labels actin filaments in the cortical ooplasm and in the follicle cell layer. β-catenin localizes to the oocyte cortex or membrane in stage II oocytes of WT and *dchs1b* mutants.
F. Hematoxylin and Eosin (H&E) stained ovary sections of WT and maternal *dachsous* mutant ovaries reveal a normal composition of oocytes. The primary oocytes of WT and *Mdchs* mutant ovaries are polarized as indicated by the presence of the Balbiani body (Bb) in stage Ib oocytes. Cortical granules begin to accumulate in stage II (II) oocytes of WT and *Mdchs* mutants and localize to the cortex in stage III (III) oocytes, which are distinguishable by the presence of yolk granules (Ygs). The structure of the vitelline envelope (VE) surrounding the oocyte is indistinguishable between WT and mutants. Images are representative of oocytes from 3 WT and 3 mutant females examined.
G. WT and *dchs1b* mutant oocytes stained with an antibody against acetylated α-tubulin.

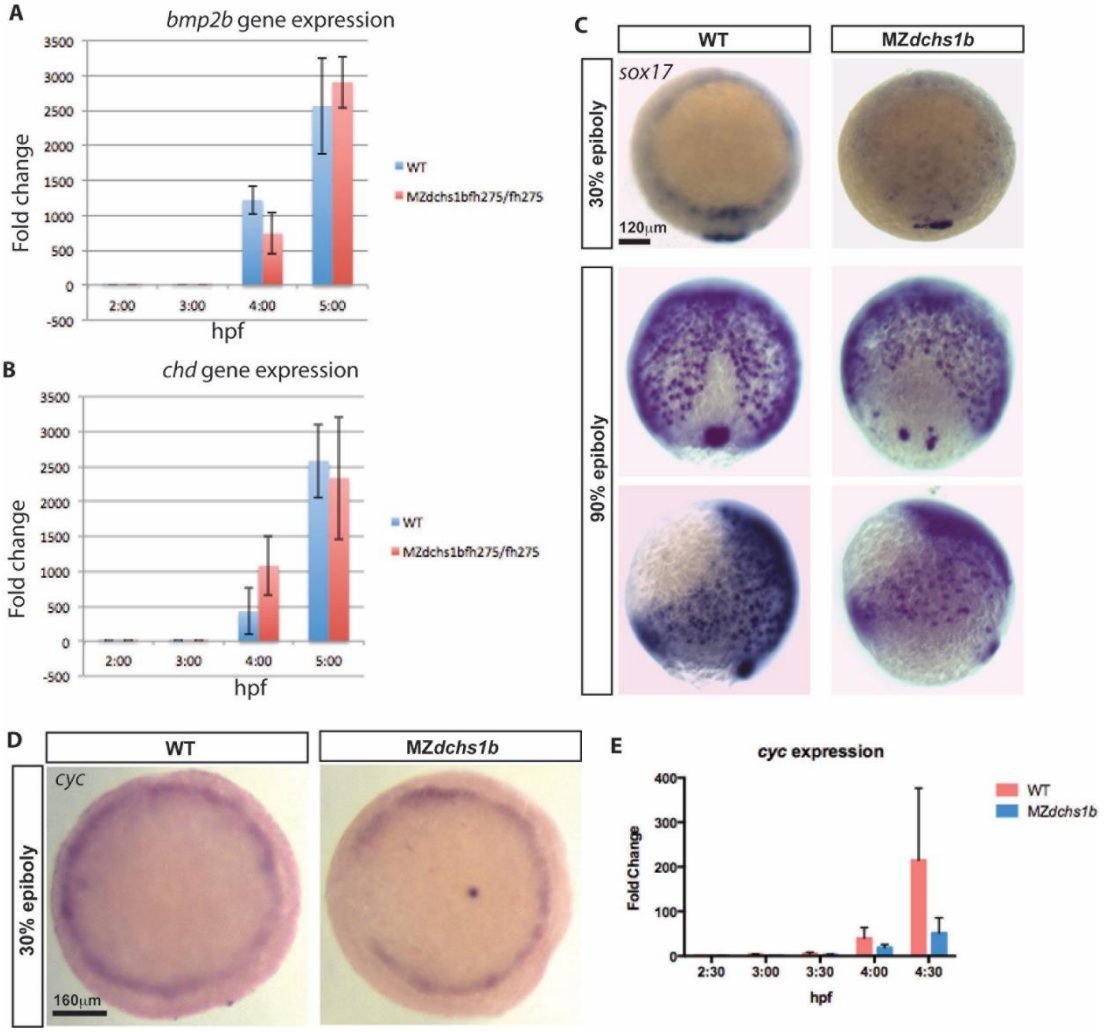

Figure S3. Levels and patterns of zygotic gene expression.

A. Expression of zygotic gene *bmp2b* in WT and MZ*dchs1b* embryos during MBT by qRT-PCR.
B. Expression of zygotic gene *chd* in WT and MZ*dchs1b* embryos during MBT by qRT-PCR.
C. Expression of *sox17* revealed by WISH in stage matched WT andMZ*dchs1b* embryos at 30% and 90% epiboly. Animal pole view for 30% epiboly embryos. Dorsal and later views for 90% epiboly embryos.
D. *cyc* WISH of stage matched WT and MZ*dchs1b* embryos; animal pole view.
E. Quantitative RT-PCR of *cyc* for time matched WT and MZ*dchs1b* embryos during MBT.

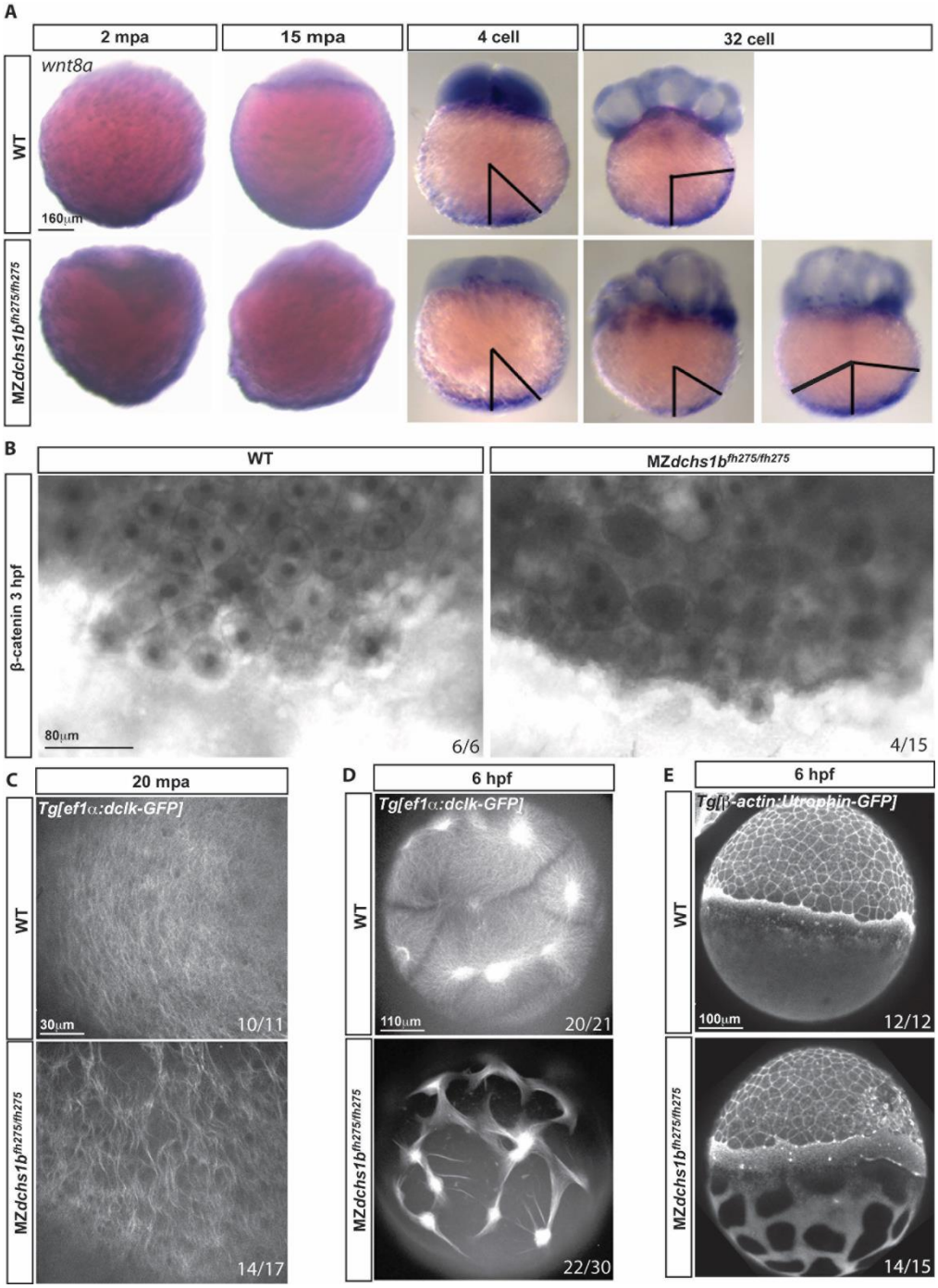

Figure S4. *wnt8a* transport and the cytoskeleton.

A. *wnt8a* transcripts detected by WISH in WT and MZ*dchs1b*$^{fh275/fh275}$ embryos at 2 mpa, 15 mpa, 4 and 32 cell stages. Representative patterns of *wnt8a* RNA expression domain in MZ*dchs1b*$^{fh275/fh275}$ embryos at 32-cell stage. Black bars mark the angle of the edge of the *wnt8a* RNA expression domain from the vegetal pole.
B. β-catenin labeling in 3 hpf WT and MZ*dchs1b*$^{fh275/fh275}$ embryos.
C. Max *z*-projection of parallel array microtubule at 20 mpa in WT and MZ*dchs1b*$^{fh275/fh275}$embryos.
D. Max *z*-projection of vegetal pole microtubule at 6 hpf in WT and MZ*dchs1b*$^{fh275/fh275}$embryos.
E. Max *z*-projection of lateral view actin at 6 hpf in WT and MZ*dchs1b*$^{fh275/fh275}$embryos.

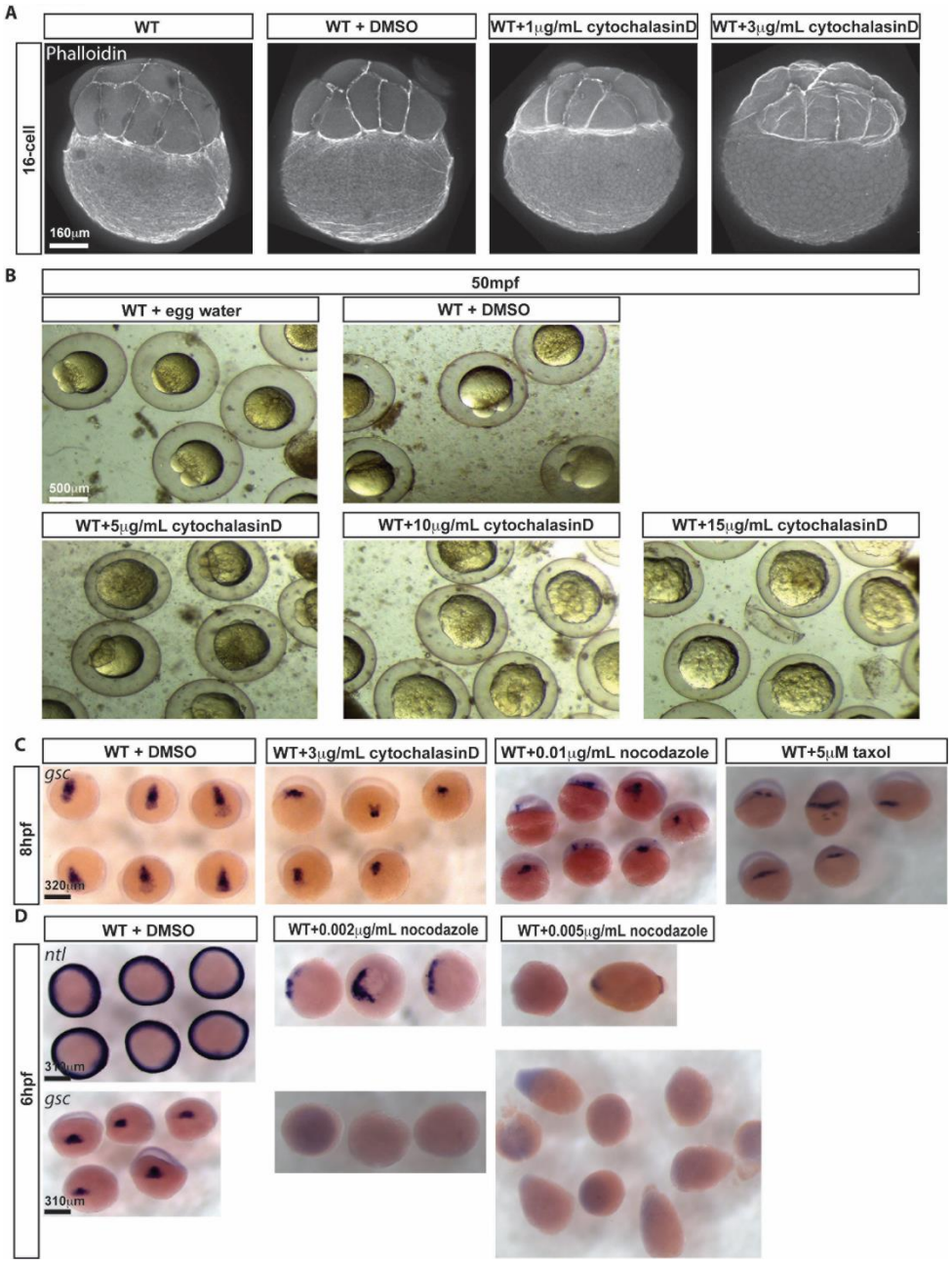

Figure S5. WT embryos treated with cytoskeleton altering agents.

A. Phalloidin labeling of F-actin at 16-cell stage for WT, WT treated with DMSO, WT treated with 1μg/mL cytochalasinD, and WT treated with 3μg/mL cytochalasinD from activation.
B. Bright field images of WT *in vitro* fertilized embryos in egg water, DMSO, 5μg/mL cytochalasinD, 10μg/mL cytochalasinD, and 15μg/mL cytochalasinD from activation at 50mpf.
C. *gsc* transcripts revealed by WISH in WT embryos treated at 1 hpf with DMSO, 3μg/mL cytochalasinD, 0.01μg/mL nocodazole, and 5μM taxol at 8 hpf; dorsal view.
D. *ntl* and *gsc* transcripts revealed by WISH in WT embryos treated at 1 hpf with DMSO, 0.002μg/mL nocodazole, and 0.005μg/mL nocodazole; 6 hpf animal pole view.

Movie S1. Chorion expansion in WT and MZ*dchs1b*$^{fh275/fh275}$ mutants.

Time-lapse imaging of WT and MZ*dchs1b*$^{fh275/fh275}$ mutants beginning at 40 seconds post activation with interval of 10 seconds for 4 minutes.

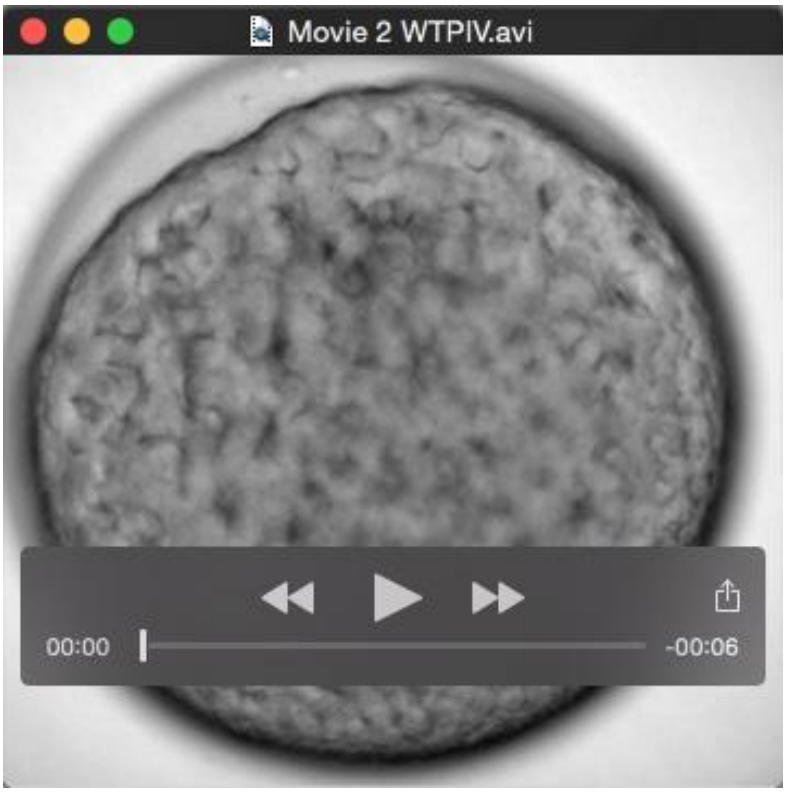

Movie S2. Representative of PIV analysis of WT embryo.

Time-lapse imaging of WT embryo beginning at 8 mpf with interval of 1 minute for 45 minutes. PIV analysis overlay bright field imaging. Red->animal pole ward. Blue->vegetal pole ward.

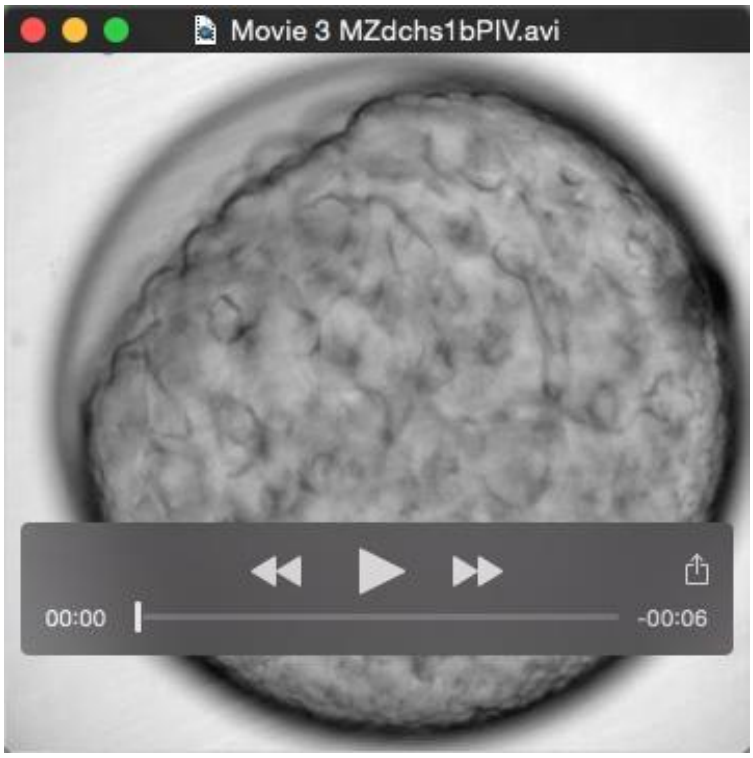

Movie S3. Representative of PIV analysis of MZ*dchs1b*$^{fh275/fh275}$ embryo.

Time-lapse imaging of MZ*dchs1b*$^{fh275/fh275}$ embryo beginning at 8 mpf with interval of 1 minute for 45 minutes. PIV analysis overlay bright field imaging. Red->animal pole ward. Blue->vegetal pole ward.

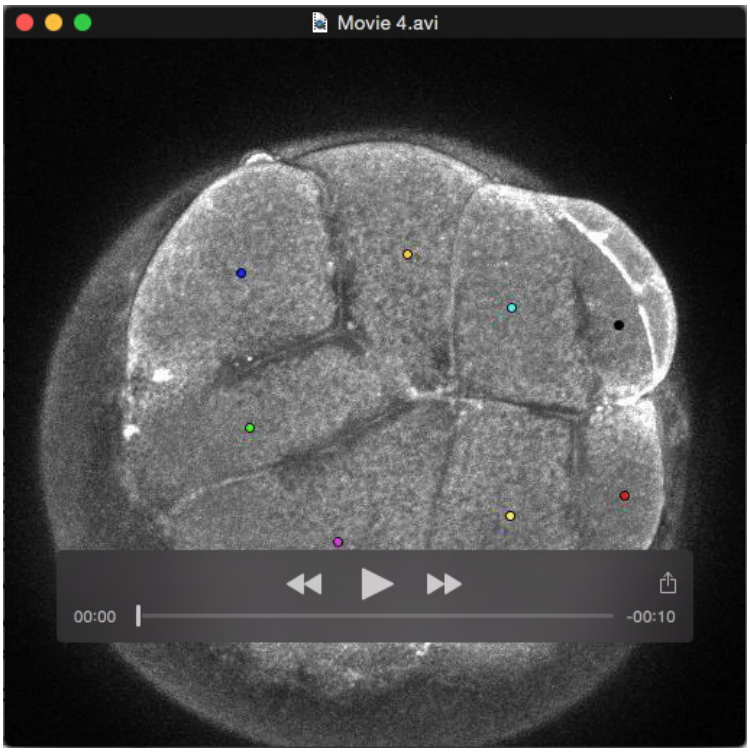

Movie S4. Cell division in MZ*dchs1b*$^{fh275/fh275}$embryo.

Time-lapse imaging of MZ*dchs1b*$^{fh275/fh275}$;*Tg[β-actin:Utrophin-GFP]* embryo beginning at 8 cells with interval of 2 minute for 31 minutes. Lineage trace indicated by color of dots. Abnormal cell divisions indicated with outlining.

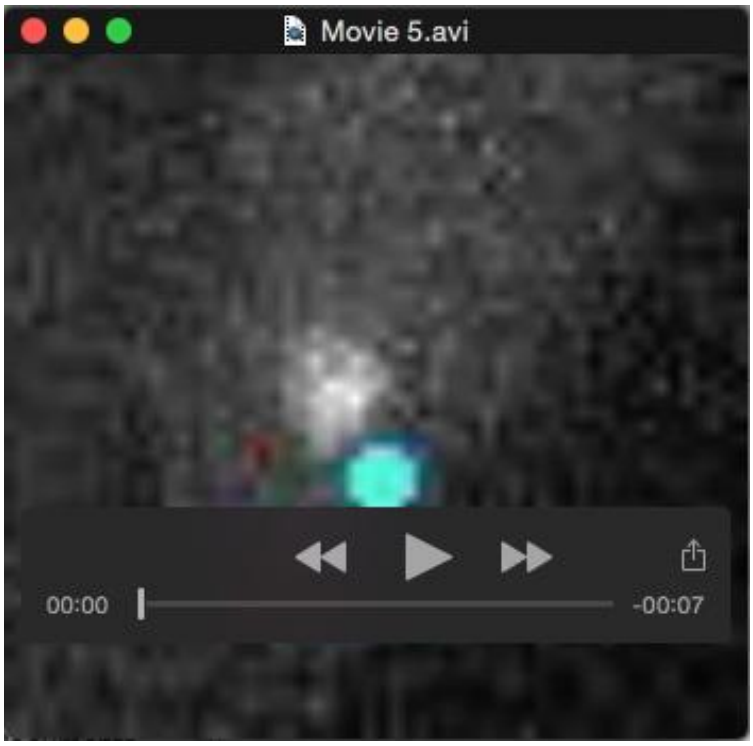

Movie S5. Single abnormal cell division in MZ*dchs1b*$^{fh275/fh275}$embryo.

Time-lapse imaging of MZ*dchs1b*$^{fh275/fh275}$embryo injected with H2B-GFP beginning at 32 cells with interval of 1 minute for 22 minutes. Lineage trace indicated by color of dots.